

# Improvement of horizontal streak on disparity map through parameter optimization for stereo vision algorithm

Melvin Gan Yeou Wei<sup>1,2</sup>, Rostam Affendi Hamzah<sup>1</sup>, Nik Syahrim Nik Anwar<sup>2</sup>,  
Adi Irwan Herman<sup>3</sup>, Jamil Abedalrahim Jamil Alsaydeh<sup>1</sup>

<sup>1</sup>Fakulti Teknologi Kejuruteraan Elektrik and Elektronik, Universiti Teknikal Malaysia Melaka, Melaka, Malaysia

<sup>2</sup>Fakulti Kejuruteraan Elektrik, Universiti Teknikal Malaysia Melaka, Melaka, Malaysia

<sup>3</sup>Product and Test Engineering, Texas Instruments, Batu Berendam, Malacca, Malaysia

## Article Info

### Article history:

Received Mar 9, 2024

Revised Apr 29, 2024

Accepted May 6, 2024

### Keywords:

Absolute differences

Gradient matching

Horizontal streak

Minimum spanning tree

Parameter optimization

Stereo vision

## ABSTRACT

In this paper, an improved local based stereo vision disparity map (SVDM) algorithm is proposed. The proposed local based SVDM algorithm include four stages and they are matching cost computation, cost aggregation disparity optimization and disparity refinement. The matching cost computation started by combining pixel to pixel matching techniques, which are absolute difference (AD) and gradient matching (GM) in producing the initial disparity map. Next, the cost aggregation uses minimum spanning tree (MST) segmentation, which equipped with edge preserving properties and noise filtering. Then, disparity optimization uses local approach with winner-take-all (WTA) technique. At the final stage, disparity refinement uses bilateral filter (BF) with weighted median (WM), which can improve the disparity map through noise removing and edges preserving. Then, the research continues to optimize the proposed local based SVDM algorithm through parameters optimization in obtaining the final disparity map. Here, multiple parameters from the proposed SVDM algorithm are manipulated and they are constant values for GM and several constant parameters in BF. By selecting the optimum parameter values, the performance of the proposed SVDM algorithm increased, especially robustness towards the horizontal streaks.

This is an open access article under the [CC BY-SA](https://creativecommons.org/licenses/by-sa/4.0/) license.



## Corresponding Author:

Rostam Affendi Hamzah

Fakulti Teknologi Kejuruteraan Elektrik dan Elektronik, Universiti Teknikal Malaysia Melaka

76100 Durian Tunggal, Melaka, Malaysia

Email: rostamaffendi@utem.edu.my

## 1. INTRODUCTION

The proposed local based stereo vision disparity map (SVDM) algorithm is organized into four stages which are matching cost computation, cost aggregation, disparity optimization and disparity refinement. At matching cost computation, pixel to pixel matching such as absolute difference (AD), squared difference (SD) and gradient matching (GM) are computational simple and fast and, but the disparity maps often highly unfavourable. To increase the robustness of matching techniques, many researchers have proposed on the blending of multiple matching techniques such as in [1], combines speeded up robust features (SURF) feature matching and census transform. Budiharto *et al.* [2] also proposed matching technique that combined weighted census transform (CT) and weighted sum of absolute difference (SAD). Finally, Winarno *et al.* [3] also proposed matching technique that combine rank transform (RT) and sum of squared difference (SSD). In this research, AD and GM techniques are combined to produce the initial disparity map. Here, the stereo image pairs (left image and right image) corresponded with each other and

produce the initial disparity map. During the matching phase, two pixel-based matching techniques undergo the corresponding process respectively. Then, their respective matching cost volumes combine to form a new initial disparity map. Next, cost aggregation uses minimum spanning tree (MST) segmentation. Cost aggregation is often curial as the initial cost of a support region is aggregated to produce disparity map with better accuracy. The initial disparity maps from matching process are often full of noise. In order to produce accurate disparity map for cost aggregation technique, comparative study from [4] reveals that adding support weight (weight) on the support region (support window) for cost aggregation technique produced good disparity map. Besides that, edge-preserving techniques also produce good disparity maps, such as bilateral filter (BF), a technique that smooth image and preserving the edges but often cause blurring to the image. Vedamurthy *et al.* [5] reveals that this technique can be traced back to the work of [6] on nonlinear gaussian filter. It was later rediscovered by [7] for the SUSAN framework and later reintroduces as BF. Another edge preserving technique that performed well is guided filter, introduced by Yang [8]. They proposed a new image filter that has edge preserving and smoothing properties like BF, yet avoid gradient reversal artefacts. The article also shows that guided filter is both effective and efficient in noise reduction, detail smoothing, HDR compression, image feathering, haze removal and joint sampling [9]. The edge preserving properties had play an important role in producing good disparity map and hence, the interest towards segmentation technique which also provide edge preserving properties [10].

The segmentation technique applied in the proposed SVDM algorithm is MST segmentation. Segmentation technique work by separating or categorizing the disparity map is into many regions. The construction of MST algorithm for this research is based on the implementation of [11]. Here, for the proposed SVDM algorithm, only MST clustering method or forest clustering was use during the aggregation of the disparity map. Disparity optimization normalized the function by selecting a disparity level and there are three approaches, such as local based, global based and semi global approach. Global based algorithm defines global energy function using technique such as dynamic programming (DP) [12], scanline optimization (SO) [13], simulated annealing (SA) [14] and graph cut (GC) [15]. Although global approach often skips cost aggregation, but complexity of the algorithm is the reason it remains unpopular at that time. Then, semi-global based algorithm combines both local based technique and global based technique, implemented by Hirschmüller *et al.* [16]. For the proposed SVDM algorithm, winner-take-all (WTA) technique is applied on the framework, making this SVDM algorithm local based. The objective of this stage is to standardize or normalize the disparity values. By using the WTA approach, the algorithm will assign minimum disparity value to each pixel of the disparity map locations [17]. Disparity refinement helps to refine the final disparity map thorough peaks removing, consistency checking, interpolating, and increasing accuracy [18]. Here, refinement stage started with post-processing, which includes left-right (LR) consistency checking process and gap filling-in. These processes are exclusively for invalid pixel detection on the occlusion region or due to mismatched process. First, the mismatched invalid pixels are identified using LR consistency checking process. Then, gap filling-in is applied to replace the mismatched invalid pixel with a valid minimum pixel value. After post processing stage is completed, the SVDM algorithm continues with disparity refinement stage, where BF with weighted median (MW) is applied to reduce the noise in the disparity maps. The refinement stage starts with an edge preserving filter namely the BF and followed by histogram equalization and finally the WM filter. The gaps of experimentations do not end here, the proposed SVDM algorithm still can be improved thru parameters optimization process. This process manipulates all parameters used in the proposed SVDM algorithm through optimizing their values. At each change, the quantitative results; average nonocc (avg nonocc) error and average all (avg all) error are obtained by uploading the disparity map results thru the Middlebury Stereo database. This database is a standard online benchmarking dataset which have been used widely by the researchers.

## 2. METHOD

### 2.1. Matching cost computation

The matching cost computation combines two pixel-based matching techniques, AD+GM. First, the matching process starts with AD, proposed by [19]. AD technique is introduced in (1),

$$AD(x, y, d) = |(I_l(x, y) - I_r(x - d, y))| \quad (1)$$

where  $(x, y)$  represents the coordinates for pixel of interest and  $d$  represents disparity value. Next,  $I_l$  represents left image and  $I_r$  represents right image. Then, AD matching is enhanced by adding a threshold which resulting to truncate the AD,  $tAD(x, y, d)$  implemented [19].  $tAD(x, y, d)$  is introduced in (2),

$$tAD(x, y, d) = \begin{cases} \tau_{AD} & , \text{ if } AD(x, y, d) > \tau_{AD} \\ AD(x, y, d) & , \text{ otherwise} \end{cases} \quad (2)$$

where  $\tau_{AD}$  represents the threshold value for AD, often for removing the outlier peak value. The second pixel-based matching technique is GM, proposed by [20]. GM matching works by extracting gradient value from the pixel of input images (left image and right image). The gradient value of horizontal direction,  $G_x$  is introduced at (3) and the gradient value of vertical direction,  $G_y$  is introduced in (4),

$$G_x = [1 \quad 0 \quad -1] * I \quad (3)$$

$$G_y = \begin{bmatrix} 1 \\ 0 \\ -1 \end{bmatrix} * I \quad (4)$$

where the  $I$  represents the targeted image and  $*$  represents the convolution operation. The gradient values from  $G_x$  and  $G_y$  enable the formation of gradient magnitude,  $m$  and is introduced in (5).

$$m = \sqrt{G_x^2 + G_y^2} \quad (5)$$

Continued from (5), a modulus operation is implemented on the gradient. The gradient displacement of x-direction and the static position of y-direction resulted to GM,  $GM(x, y, d)$  and is introduced in (6),

$$GM(x, y, d) = |m_l(x, y) - m_r(x - d, y)| \quad (6)$$

where  $(x, y)$  represents the coordinates of pixel of interest,  $d$  represents disparity value,  $m_l$  represents gradient value for left image and  $m_r$  represents the gradient value for right image. Then GM matching is also enhanced by adding a threshold resulting to truncated GM,  $gGM(x, y, d)$  and introduced in (7),

$$gGM(x, y, d) = \begin{cases} \tau_{GM} & , \text{ if } GM > \tau_{GM} \\ GM & , \text{ otherwise} \end{cases} \quad (7)$$

where  $\tau_{GM}$  represents the threshold value, aiding in peaks removing. The combination for  $tAD(x, y, d)$  and  $GM(x, y, d)$ , resulted to final form of matching cost function,  $MCC(p, d)$  and introduce in (8),

$$MCC(p, d) = tAD(p, d) + \alpha [gGM(p, d)] \quad (8)$$

where  $p$  represents  $(x, y)$ ; the coordinates for pixel of interest and  $\alpha$  represents the constant value which is sensitivity manipulator for illumination differences.

## 2.2. Cost aggregation

The cost aggregation of SVDM algorithm uses MST segmentation, contributed by [21] and well-known for its edge preserving properties. MST and color image segmentation framework is presented as following,

- i) Spanning tree, a non-orientation graph of object has an equation of  $G = [V, E]$ , where  $V$  represents a set of vertices that corresponds to the data set,  $E$  represents edge that link to the vertices, and  $e_m = (x_i, x_j)$  represents each edge that connects to a pair of vertices. The MST,  $G$  is introduced in (9).

$$\begin{aligned} MST &= (A, T) | A = V, T = \{e_1, \dots, e_{n-1}\} \\ m(MST) &= \min\{m(tree) | tree = (V, T')\} \end{aligned} \quad (9)$$

- ii) By adding  $d_y$ , a cut-off point, edges where weights are greater than the cut-off point are eliminated from MST, forming the forest,  $F$  of  $V$  and is introduced in (10).

$$F = \{(V, E') | E' = T - \{e' | m(e') > d_y\}\} \quad (10)$$

- iii) The accumulation for all the trees into  $F$  is presented in (11).

$$\{(V_i, T_i) | i = 1, 2, \dots, m\}, F = \cup_{i=1}^m (V_i, T_i) \tag{11}$$

where,  $\cup_{i=1}^m V_i = V, \cup_{i=1}^m T_i = E'$

iv) Each  $(V_i, T_i)$  could be assume as a cluster  $C_i = X_i$ , where  $T_i = \cup_k (e_k' | e' < d_y)$

The function of matching cost computation,  $MCC(p, d)$ , from matching process will represents the set of vertices that corresponds to the data set for spanning tree equation,  $G = [V, E]$ . By replacing  $MCC(x, y, d)$  into V, in (12) is introduced.

$$G = [MCC(p, d), E] \tag{12}$$

The spanning tree equation represents the cost aggregation process, hence the cost aggregation equation,  $CA(p, d)$  is introduced as (13).

$$CA(p, d) = [MCC(p, d), E] \tag{13}$$

**2.3. Disparity optimization**

The disparity optimization applied the local approach; hence, WTA technique is used. By using WTA, implemented by [22], [23], each pixel at disparity map are normalized through minimum disparity value. WTA is presented in (14):

$$d(p, d) = arg \min_{d \in D} CA(p, d) \tag{14}$$

where  $d(p)$  represents disparity value at the coordinate of  $(x, y)$ ,  $D$  represents range of disparity on an image and  $CA(p, d)$  represents data obtain from previous stage, cost aggregation for this research.

**2.4. Disparity refinement**

The disparity refinement stage uses BF with WM. There are two processes; post-processing and disparity refinement. In general, post processing, implemented by [24] and [25], involves left right (LR) consistency checking and gap filling-in. LR checking works by detecting outlier, where the procedure begins from left reference disparity map image that coincides with the right reference of disparity map. The mismatched values among the two images are declared as invalid pixel. LR checking is introduced in (15).

$$|d_{LR}(p) - d_{RL}(p - d_{LR}(p))| \leq \tau_{LR} \tag{15}$$

where,  $d_{LR}(p)$  represents disparity map with the coordinate of left reference and  $d_{RL}(p - d_{LR}(p))$  represents disparity map with the coordinate of right reference. Then,  $\tau_{LR}$  represents the cut-off point for  $d_{LR}(p)$ . The filling-in process interpolated the gaps which contains the invalid pixels with mismatched disparity value. Then, the gaps are identified and replaced with the nearest valid disparity value. Furthermore, the valid value is set to be position at the same scanning line. The gap filling-in process is introduced in (16),

$$d(p) = \begin{cases} d(p - i), & d(p - i) \leq d(p + j), \\ d(p + j), & otherwise \end{cases} \tag{16}$$

where  $d(p)$  is disparity value of coordinate  $p$ . Next,  $(p - i)$  is the position of the first valid disparity on the left side and  $(p + j)$  is the coordinate of the first valid disparity on the right side. After post-processing, disparity refinement begins with BF. This is often done to remove remaining noises lingering in the disparity map.,  $BF(p, q)$  proposed by [26] is introduced in (17),

$$BF(p, q) = exp\left(-\frac{|p-q|^2}{\sigma_s^2}\right) exp\left(-\frac{|d(p)-d(q)|^2}{\sigma_c^2}\right) \tag{17}$$

where  $(p, q)$  represents the coordinate for target pixel and neighbouring pixels. Next,  $|p - q|$  represents spatial Euclidean and  $|d(p) - d(q)|^2$  represents Euclidean [27]. Then,  $\sigma_s^2$  represents spatial distance and  $\sigma_c^2$  represents colour similarity. BF also consist of edge preserving properties and this enable further improve on the disparity map. The  $BF(p, q)$  is then transformed into histogram equalization,  $h(p, d_r)$  and introduced in (18),

$$h(p, d_r) = \sum_{q \in w_p | d(q) == d_r} BF(p, q) \tag{18}$$

where  $d_r$  represents disparity range and  $w_p$  represents window size with the radius ( $r \times r$ ) at centred pixel of  $p$ . WM is then implemented for further improvement, proposed by [28]. The final equation for disparity map, are WM towards histogram equalization,  $h(p, d_r)$  and is introduced in (19).

$$WM = med\{d|h(p, d_r)\} \quad (19)$$

### 3. RESULTS AND DISCUSSION

The proposed SVDM algorithm is optimized through manipulating 4 parameters and they are  $\alpha, \sigma_s, \sigma_c$  and  $w_p$ . Table 1 presents the manipulated parameters and their respective equation. At each increment or decrement, the final disparity maps are uploaded to Middlebury stereo evaluation system with quantitative results; average nonocc (avg nonocc) error and average all (avg all) error.

Algorithm stage	Equation for parameter manipulation	Parameters
Stage 1	Combined matching cost; $CM(p, d)$ : $MCC(p, d) = tAD(p, d) + \alpha [gGM(p, d)]$	$\alpha$
Stage 4	Bilateral filter; $B(p, q)$ : $BF(p, q) = exp\left(-\frac{ p - q ^2}{\sigma_s^2}\right) exp\left(-\frac{ d(p) - d(q) ^2}{\sigma_c^2}\right)$	$\sigma_s, \sigma_c$
	Histogram equalization; $h(p, d_r)$ : $h(p, d_r) = \sum_{q \in w_p   d(q) = d_r} BF(p, q)$	$w_p$

#### 3.1. Parameter optimization for $\alpha$

This subsection indicates the impact of varying the  $\alpha$  parameter on the results. Building upon the previous value, the  $\alpha$  value is increased by 0.1 until it reaches at 11.00. Table 2 displays the results, indicating that an  $\alpha$  value of 10.7 at E8 resulted in the highest accuracy. This was accompanied by an average nonocc error of 9.46% and an average all error of 12.8%.

Error (%)	E1	E2	E3	E4	E5	E6	E7	E8	E9	E10	E11
$\alpha$	10.00	10.10	10.20	10.30	10.40	10.50	10.60	10.70	10.80	10.90	11.00
Avg nonocc	9.53	9.49	9.47	9.48	9.49	9.48	9.47	<b>9.46</b>	9.46	9.47	9.46
Avg all	13.00	12.90	12.90	12.90	12.90	12.90	12.90	<b>12.80</b>	12.90	12.90	12.90

#### 3.2. Parameter optimization for $\sigma_s$

Picking up from previous value,  $\sigma_s$  at 16.0 is further manipulated through continuous decrement of 0.01 until  $\sigma_s$  reaches 15.0. Tabulated results at Table 3 shows  $\sigma_s$  valued at 15.8, that is the first to achieve the highest accuracy, when comparing to  $\sigma_s$  at 15.9 and 16.0. The avg nonocc error is 7.65% and the avg all error is 10.9%.

Error (%)	E1	E2	E3	E4	E5	E6	E7	E8	E9	E10	E11
$\sigma_s$	15.00	15.10	15.20	15.30	15.40	15.50	15.60	15.70	15.80	15.90	16.00
Avg nonocc	7.68	7.67	7.67	7.67	7.67	7.67	7.66	7.66	<b>7.65</b>	7.65	7.65
Avg all	10.90	10.90	10.90	10.90	10.90	10.90	10.90	10.90	<b>10.90</b>	10.90	10.90

#### 3.3. Parameter optimization for $\sigma_c$

This subsection specifies the  $\sigma_c$  values which starts with 0.170 at E1. Table 4 presents the values of  $\sigma_c$  at different levels with 0.001 increment. Among these values (i.e., specifically 0.175, 0.176, 0.177, 0.178, and 0.179), 0.175 is the first to achieve the highest accuracy. The average nonocc error is reported to be 7.61%, while the average all error is 10.8% at E6.

Table 4. Avg nonocc error and avg all error for further parameter manipulation of  $\sigma_c$

Error (%)	E1	E2	E3	E4	E5	E6	E7	E8	E9	E10	E11
$\sigma_c$	0.170	0.171	0.172	0.173	0.174	0.175	0.176	0.177	0.178	0.179	0.180
Avg nonocc	7.61	7.61	7.61	7.61	7.61	<b>7.61</b>	7.61	7.61	7.61	7.61	7.61
Avg all	10.9	10.9	10.9	10.9	10.9	<b>10.8</b>	10.8	10.8	10.8	10.8	10.9

### 3.4. Parameter optimization for $w_p$

The experiment first started by setting  $w_p$  at 11×11 until 39×39, resulting to several samples of data. Based on Table 5,  $w_p$  at 1×1 has the highest error, where avg nonocc error is 8.97% and avg all error is 12.3%. However, by selecting the optimum size for  $w_p$  is slightly different, due to the differences in assumption when obtaining the highest accuracy for avg nonocc error and avg all error. For avg nonocc error,  $w_p$  at 21×21 attained the highest accuracy, 7.53%, but for avg all error, there are multiple options, such as  $w_p$  at 31×31, 33×33, 37×37, and 39×39. All attained the highest accuracy of 10.6%. Here comes the conflict, as the best results for avg nonocc error and avg all error does not tally with each other. Therefore,  $w_p$  at 31×31 is selected, for first attaining the highest accuracy for avg all error, valued at 7.58% and avg nonocc error at 7.58%. Then, through Middlebury stereo dataset, Table 6 presents quantitative results, which include the nonocc error and all error for the final disparity maps. Furthermore, the avg nonocc error is 7.58% and avg all errors 10.6%.

Table 5. Avg nonocc error and avg all error for parameter manipulation of  $w_p$

$w_p$	1	3	5	7	9	11	13	15	17	19	21	23	25	27	29	31	33	35	37	39
Avg nonocc	8.97	8.26	7.97	7.81	7.70	7.61	7.59	7.56	7.55	7.56	7.53	7.54	7.54	7.55	7.57	<b>7.58</b>	7.58	7.61	7.61	7.60
All	12.3	11.5	11.2	11.1	11.0	10.8	10.8	10.8	10.8	10.9	10.7	10.7	10.7	10.7	10.7	<b>10.6</b>	10.6	10.7	10.6	10.6

Table 6. The nonocc error and all error comparison

Error (%)	Weight avg	Adiron	ArtL	Jadepl	Motor	MotorE	Piano	PianoL	Pipes	Playrm	Playt	PlaytP	Recyc	Shelvs	Teddy	Vintge
Nonocc	7.58	4.88	6.81	15.3	4.24	7.42	5.82	12.7	7.26	8.12	17.1	4.12	4.43	11.0	3.38	13.4
All	10.6	5.92	12.4	30.2	6.52	9.24	6.44	13.0	12.2	13.2	19.5	4.94	4.66	11.2	4.79	14.3
Nonocc [24]	11.3	18.3	7.45	15.7	3.48	29.1	6.51	38.4	5.37	12.8	13.5	3.24	3.44	15.1	3.00	11.1
All [24]	18.9	21.1	17.8	38.7	11.0	36.4	11.6	40.0	13.6	25.4	20.0	8.74	5.97	17.6	10.7	18.3

### 3.5. Parameter optimization reduces horizontal streaks

In stereo matching, common limitations and challenges are the matching on low texture regions, repetitive regions, depth discontinuity, illumination difference and occlusion. However, in this article, one of the unique challenges encountered, especially pre-optimization process is horizontal streaking problem. Figure 1 provides some samples for parameters optimization process. Out of 15 samples from the Middlebury Stereo, only three set of results regarding the parameter optimization process are included here, and they are from Adirondack, MotorcycleE, and Recycle. The parameter values are optimized values, acquired from the finding of parameter optimization process. The qualitative results (disparity maps) and quantitative results (all errors) are also presented in Figure 1. The pre-optimization process, where  $\alpha$  at 1.0,  $\sigma_s$  at 1.0,  $\sigma_c$  at 0.10 and  $w_p$  at 11×11, shows that the disparity maps are heavily affected by horizontal streaks. The all errors are 19.3%, 38.1%, and 6.51 % respectively for Adirondack, MotorcycleE, and Recycle. However, by manipulating the constant,  $\alpha$  for GM, from 1.0 to 10.7, there are vivid improvements on the results. The three disparity maps (Adirondack, MotorcycleE, and Recycle) show massive reduction on horizontal streaks and in correspond, all error is also reduced. The respective all errors are 12.8%, 13.5%, and 5.69% for Adirondack, MotorcycleE, and Recycle. Here, quantitatively, MotorcycleE experience the biggest improvement, from 38.1% to 13.5%, drastically reduced to 24.6%. The parameters optimizing process then continued by manipulating the parameter or elements of BF. The first element,  $\sigma_s$  is referring to spatial distance for BF is manipulated from 1.0 to 15.8 and there is improvement on the results. Three disparity maps show nearly reduction of horizontal streaks and leaving behind salts and peppers of invalid pixels. For upcoming development, the vertical streaks which is also accured in disparity map could be resolved if parameter optimization process is utilized.

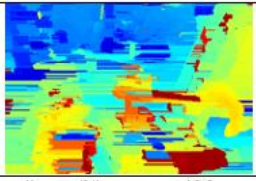
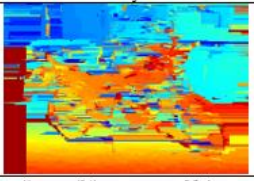
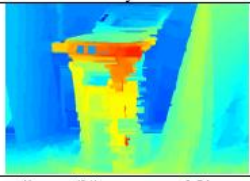
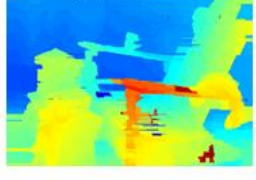
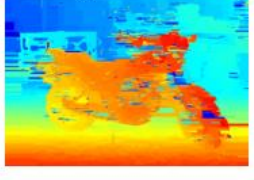
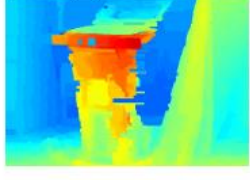
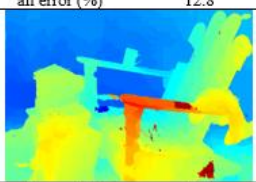
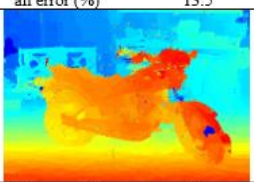
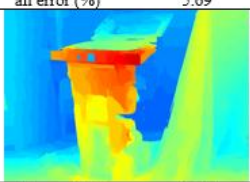
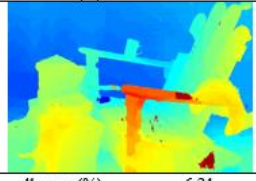
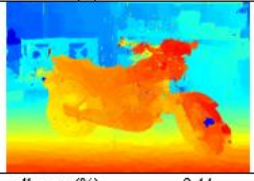
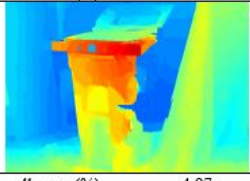
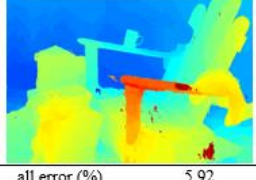
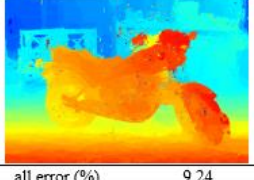
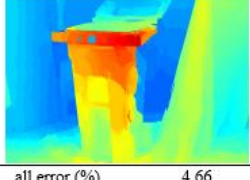
Parameter values	Disparity map		
	Adirondack	MotorcycleE	Recycle
$\alpha=1.0$ $\sigma_s=1.0$ $\sigma_c=0.10$ $w_p=11\times 11$			
	all error (%) 19.3	all error (%) 38.1	all error (%) 6.51
$\alpha=10.7$ $\sigma_s=1.0$ $\sigma_c=0.10$ $w_p=11\times 11$			
	all error (%) 12.8	all error (%) 13.5	all error (%) 5.69
$\alpha=10.7$ $\sigma_s=15.8$ $\sigma_c=0.10$ $w_p=11\times 11$			
	all error (%) 6.31	all error (%) 9.54	all error (%) 4.98
$\alpha=10.7$ $\sigma_s=15.8$ $\sigma_c=0.175$ $w_p=11\times 11$			
	all error (%) 6.21	all error (%) 9.44	all error (%) 4.97
$\alpha=10.7$ $\sigma_s=15.8$ $\sigma_c=0.175$ $w_p=31\times 31$			
	all error (%) 5.92	all error (%) 9.24	all error (%) 4.66

Figure 1. Results of improvement for parameter optimization

In addition, all errors also reduce to 6.31%, 9.54%, and 4.98% respectively among the three disparity maps. Next, the second element  $\sigma_c$ , referring to colour similarity for BF is manipulated from 0.10 to 0.175. Here there are minor improvement. For three disparity maps, there are minor reduction on invalid pixels and validated by the minor reduction in all errors. The respectively all errors are 6.21%, 9.44%, and 4.97% among the three disparity maps. Lastly, the third element  $w_p$ , referring to window size for BF is manipulated from  $11\times 11$  to  $31\times 31$ . Here there are also minor improvement with 5.92%, 9.24%, and 4.66% for three disparity maps respectively. Hence, the parameter optimization process improved the accuracy of the proposed SVDM algorithm. In addition, in this experiment, especially the parameter optimization process for  $\alpha$  and  $\sigma_s$  (constant for GM and spatial distance for BF), contribute greatly to reducing horizontal streaks.

#### 4. CONCLUSION

Based on this study, the parameter optimization process is capable to improve the disparity map quality. The horizontal streak or noise on the disparity maps are reduced and the quantitative measurement demonstrate the increment of accuracy. Hence, this process is very important which proper selection of a constant parameter in every framework stage could produce results that are more accurate. This is proved by experimental analysis on matching cost computation and disparity refinement stage with four different constant parameter selections. Referring to the experimental results, the Adirondack, Motorcycle, and Recycle images show improvement on the horizontal streak from an early stage of parameter settings until at the final results. For example, the improvement of Motorcycle image almost 28% of noise reduction. It expresses the parameter optimization process that is significant to determine the best results.

**ACKNOWLEDGEMENTS**

This research project is supported by the Universiti Teknikal Malaysia Melaka.




**REFERENCES**

- [1] D. Scharstein, R. Szeliski, and R. Zabih, "A taxonomy and evaluation of dense two-frame stereo correspondence algorithms," in *Proceedings IEEE Workshop on Stereo and Multi-Baseline Vision (SMBV 2001)*, 2002, pp. 131–140, doi: 10.1109/SMBV.2001.988771.
- [2] W. Budiharto, A. Santoso, D. Purwanto, and A. Jazidie, "Multiple moving obstacles avoidance of service robot using stereo vision," *TELKOMNIKA (Telecommunication Computing Electronics and Control)*, vol. 9, no. 3, p. 433, Dec. 2011, doi: 10.12928/telkomnika.v9i3.733.
- [3] E. Winarno, A. Harjoko, A. M. Arymurthy, and E. Winarko, "Face recognition based on symmetrical half-join method using stereo vision camera," *International Journal of Electrical and Computer Engineering (IJECE)*, vol. 6, no. 6, pp. 2818–2827, Dec. 2016, doi: 10.11591/ijece.v6i6.pp2818-2827.
- [4] R. A. Hamzah, S. F. A. Ghani, A. Din, and K. A. A. Aziz, "Visualization of image distortion on camera calibration for stereo vision application," in *2012 IEEE International Conference on Control System, Computing and Engineering*, Nov. 2012, pp. 28–33, doi: 10.1109/ICCSCE.2012.6487110.
- [5] I. Vedamurthy *et al.*, "Recovering stereo vision by squashing virtual bugs in a virtual reality environment," *Philosophical Transactions of the Royal Society B: Biological Sciences*, vol. 371, no. 1697, p. 20150264, Jun. 2016, doi: 10.1098/rstb.2015.0264.
- [6] H. X. Haifeng Xi and W. Cui, "Wide baseline matching using support vector regression," *TELKOMNIKA (Telecommunication Computing Electronics and Control)*, vol. 11, no. 3, p. 597, Sep. 2013, doi: 10.12928/telkomnika.v11i3.1144.
- [7] S. S. N. j Bhuiyan and O. O. Khalifa, "Efficient 3D stereo vision stabilization for multi-camera viewpoints," *Bulletin of Electrical Engineering and Informatics*, vol. 8, no. 3, pp. 882–889, Sep. 2019, doi: 10.11591/eei.v8i3.1518.
- [8] Q. Yang, "A non-local cost aggregation method for stereo matching," in *2012 IEEE Conference on Computer Vision and Pattern Recognition*, Jun. 2012, pp. 1402–1409, doi: 10.1109/CVPR.2012.6247827.
- [9] C. Rhemann, A. Hosni, M. Bleyer, C. Rother, and M. Gelautz, "Fast cost-volume filtering for visual correspondence and beyond," in *CVPR 2011*, Jun. 2011, pp. 3017–3024, doi: 10.1109/CVPR.2011.5995372.
- [10] R. A. Setyawan, R. Soenoko, M. A. Choiron, and P. Mudjirahardjo, "Matching algorithm performance analysis for autocalibration method of stereo vision," *TELKOMNIKA (Telecommunication Computing Electronics and Control)*, vol. 18, no. 2, p. 1105, Apr. 2020, doi: 10.12928/telkomnika.v18i2.14842.
- [11] F. A. Phang *et al.*, "Integrating drone technology in service learning for engineering students," *International Journal of Emerging Technologies in Learning (IJET)*, vol. 16, no. 15, p. 78, Aug. 2021, doi: 10.3991/ijet.v16i15.23673.
- [12] S. Ahmed, M. Hansard, and A. Cavallaro, "Constrained optimization for plane-based stereo," *IEEE Transactions on Image Processing*, vol. 27, no. 8, pp. 3870–3882, Aug. 2018, doi: 10.1109/TIP.2018.2823543.
- [13] Y. Lee and C.-M. Kyung, "A memory- and accuracy-aware gaussian parameter-based stereo matching using confidence measure," *IEEE Transactions on Pattern Analysis and Machine Intelligence*, vol. 43, no. 6, pp. 1845–1858, Jun. 2021, doi: 10.1109/TPAMI.2019.2959613.
- [14] L. Kong, J. Zhu, and S. Ying, "Local stereo matching using adaptive cross-region-based guided image filtering with orthogonal weights," *Mathematical Problems in Engineering*, vol. 2021, pp. 1–20, May 2021, doi: 10.1155/2021/5556990.
- [15] J. Zbontar and Y. LeCun, "Computing the stereo matching cost with a convolutional neural network," in *2015 IEEE Conference on Computer Vision and Pattern Recognition (CVPR)*, Jun. 2015, pp. 1592–1599, doi: 10.1109/CVPR.2015.7298767.
- [16] H. Hirschmüller, P. R. Innocent, and J. Garibaldi, "Real-time correlation-based stereo vision with reduced border errors," *International Journal of Computer Vision*, vol. 47, no. 1–3, pp. 229–246, 2002, doi: 10.1023/A:1014554110407.
- [17] N. Ma, Y. Men, C. Men, and X. Li, "Accurate dense stereo matching based on image segmentation using an adaptive multi-cost approach," *Symmetry*, vol. 8, no. 12, p. 159, Dec. 2016, doi: 10.3390/sym8120159.
- [18] W. Yuan, C. Meng, X. Tong, and Z. Li, "Efficient local stereo matching algorithm based on fast gradient domain guided image filtering," *Signal Processing: Image Communication*, vol. 95, p. 116280, Jul. 2021, doi: 10.1016/j.image.2021.116280.
- [19] R. A. Hamzah, M. G. Y. Wei, and N. S. N. Anwar, "Stereo matching based on absolute differences for multiple objects detection," *TELKOMNIKA (Telecommunication Computing Electronics and Control)*, vol. 17, no. 1, p. 261, Feb. 2019, doi: 10.12928/telkomnika.v17i1.9185.
- [20] S.-S. Wu, C.-H. Tsai, and L.-G. Chen, "Efficient hardware architecture for large disparity range stereo matching based on belief propagation," in *2016 IEEE International Workshop on Signal Processing Systems (SiPS)*, Oct. 2016, pp. 236–241, doi: 10.1109/SiPS.2016.49.
- [21] S. Fakhar, M. Saad, A. Fauzan, R. Affendi, and M. Aidil, "Development of portable automatic number plate recognition (ANPR) system on Raspberry Pi," *International Journal of Electrical and Computer Engineering (IJECE)*, vol. 9, no. 3, pp. 1805–1813, Jun. 2019, doi: 10.11591/ijece.v9i3.pp1805-1813.
- [22] "Middlebury stereo evaluation," *Middlebury*, 2017. <https://vision.middlebury.edu/stereo/eval3/>.
- [23] N. Einecke and J. Eggert, "Anisotropic median filtering for stereo disparity map refinement," in *Proceedings of the International Conference on Computer Vision Theory and Applications*, 2013, pp. 189–198, doi: 10.5220/0004200401890198.
- [24] R. A. Hamzah, R. A. Rahim, and H. N. Rosly, "Depth evaluation in selected region of disparity mapping for navigation of stereo vision mobile robot," in *2010 IEEE Symposium on Industrial Electronics and Applications (ISIEA)*, Oct. 2010, pp. 551–555, doi: 10.1109/ISIEA.2010.5679404.
- [25] K. Zhang, J. Li, Y. Li, W. Hu, L. Sun, and S. Yang, "Binary stereo matching," in *Proceedings - International Conference on Pattern Recognition (ICPR)*, 2012, pp. 356–359, doi: 10.1109/ICPR.2012.9489043.
- [26] M. Kitagawa, I. Shimizu, and R. Sara, "High accuracy local stereo matching using DoG scale map," in *2017 Fifteenth IAPR International Conference on Machine Vision Applications (MVA)*, May 2017, pp. 258–261, doi: 10.23919/MVA.2017.7986850.
- [27] W. Mao and M. Gong, "Disparity filtering with 3D convolutional neural networks," in *2018 15th Conference on Computer and Robot Vision (CRV)*, May 2018, pp. 246–253, doi: 10.1109/CRV.2018.00042.
- [28] Y. Li and S. Fang, "Removal-based multi-view stereo using a window-based matching method," *Optik*, vol. 178, pp. 1318–1336, Feb. 2019, doi: 10.1016/j.jleo.2018.10.126.






## BIOGRAPHIES OF AUTHORS






**Melvin Gan Yeou Wei**    was born in 1992, he graduated from Universiti Teknikal Malaysia Melaka where he received his B.Eng majoring in Electrical and Master Degree in Mechatronic Engineering respectively. Currently, he is pursuing Ph.D. in the Universiti Teknikal Malaysia Melaka. He can be contacted at email: melvin.gyw92@gmail.com.






**Rostam Affendi Hamzah**    graduated from Universiti Teknologi Malaysia where he received his B.Eng majoring in Electronic Engineering. Then he received his M.Sc. majoring in Electronic System Design Engineering and Ph.D. majoring in Electronic Imaging from the Universiti Sains Malaysia. Currently he is a lecturer in the Universiti Teknikal Malaysia Melaka teaching digital electronics, digital image processing, and embedded system. He can be contacted at email: rostamaffendi@utem.edu.my.



**Nik Syahrim Nik Anwar**    was born in 1981, he graduated from University of Applied Science Heilbronn, Germany where he received his Diplom in Mechatronik und Mikrosystemtechnik majoring in Mechatronics in 2006. In 2010 he received his M.Sc. majoring in Mechatronics from the University of Applied Science Aachen, Germany. In 2018, he received Ph.D. majoring in Electrical from the Universiti Sains Malaysia. Currently he is a senior lecturer in Universiti Teknikal Malaysia Melaka teaching Electrical and Mechatronics subjects. He can be contacted at email: syahrim@utem.edu.my.



**Adi Irwan Herman**    graduated in 2015 with a Bachelor Degree in Computer Engineering Technology (Computer System) from the Universiti Teknikal Malaysia Melaka. Currently, he works with Texas Instrument more than 5 years with his current research interests are computer engineering related field of studies. He can be contacted at email: adiirwanherman@gmail.com.



**Jamil Abedalrahim Jamil Alsayaydeh**    received an M.S. degree in computer systems and networks from Zaporizhzhia National Technical University, Ukraine, in 2010 and Ph.D. in Engineering Sciences with a specialization in Automation of Control Processes from National Mining University, Ukraine, in 2014. Currently a Senior Lecturer at Universiti Teknikal Malaysia Melaka (UTeM) since 2015. Research interests include artificial intelligence, IoT, energy conservation, web service composition, and wireless mesh networks. Author/co-author of 47+ research publications cited in over 100 documents. Actively supervises students, reviews for reputable journals, secures grants, and holds membership in Board of Engineers Malaysia (BEM). He can be contacted at email: jamil@utem.edu.my.